A Collection of Conceptual Climate Models

1 Energy Balance Models

1.1 Zero-D

Very simply, the globally averaged surface temperature of the Earth may be seen as the result of the net radiative heat budget - between incoming short wave (SW) and outgoing infra red (IR) radiation. If the incoming energy per unit area at the top of the atmosphere is Q, then the total energy received by the Earth is

$$\pi R_E^2 Q(1-\alpha) \tag{1}$$

The factor πR_E^2 appears because the area of the intercepted solar radiation is that of a disk of radius R_E. The quantity α, called the planetary albedo, represents the fraction of radiation that is reflected away.

The outgoing IR radiation can be considered to be from a black body of temperature T - the globally averaged surface temperature of the Earth. By the Stefan-Boltzmann Law, the emitted radiation per unit area is σT^4, where $\sigma = 5.67 \times 10^8\ \mathrm{W\,m^{-2}\,K^{-4}}$. Multiplying by the total surface area of the earth, $4\pi R_E^2$, the net outgoing radiation is obtained -

$$4\pi R_E^2 \sigma \gamma T^4 \tag{2}$$

where γ is a greenhouse factor (whose value is less than one as greenhouse gases 'trap' incoming radation).

The rate of change of the atmospheric heat content can thus be written as

$$4\pi R_E^2 h \rho_a c_p \frac{dT}{dt} = \pi R_E^2 Q(1-\alpha) - 4\pi R_E^2 \sigma \gamma T^4 \tag{3}$$

where h is the height, ρ_a the density, and c_p the specific heat capacity of the atmosphere. The above equation can be simplified to

$$c\dot{T} = \frac{1}{4}Q(1-\alpha) - \sigma\gamma T^4 \tag{4}$$

with $c = h\rho_a c_p$. Typical values of the parameters are given in table [X].

The planetary albedo α is mainly due to the presence of ice on land and sea, and thus its value depends on the surface temperature. It is convenient to define a family of equilibrium albedo functions:

$$\alpha(T) = a_1 - \frac{1}{2}a_2\left[1 + \tanh\left(\frac{T - T^\star}{\Delta T}\right)\right] \tag{5}$$

an example of which is shown in figure [X]. Depending on the choice of albedo function and Q, more than one steady state can exist, as can be seen from figure [X]. The stability of the fixed points in the system can be analyzed by examining the phase space (figure [X]). [....]

A three-dimensional phase space, spanned by $\dot{T}, T$ and Q shows the existence of multiple equilibrium states within a range of values of Q. If Q is undergoing variations[1], then the climate system can undergo hysteresis - jumping from one stable branch to another and taking different paths along different directions of changing Q (figure [X]). The phenomena of abrupt transitions, as seen in this very simple climate model, is the basis of the Milankovitch[2] theory of ice ages.

[1] Due to quasi-periodic variations in orbital orientation

[2] Named after the Serbian mathematician Multin Milankovic

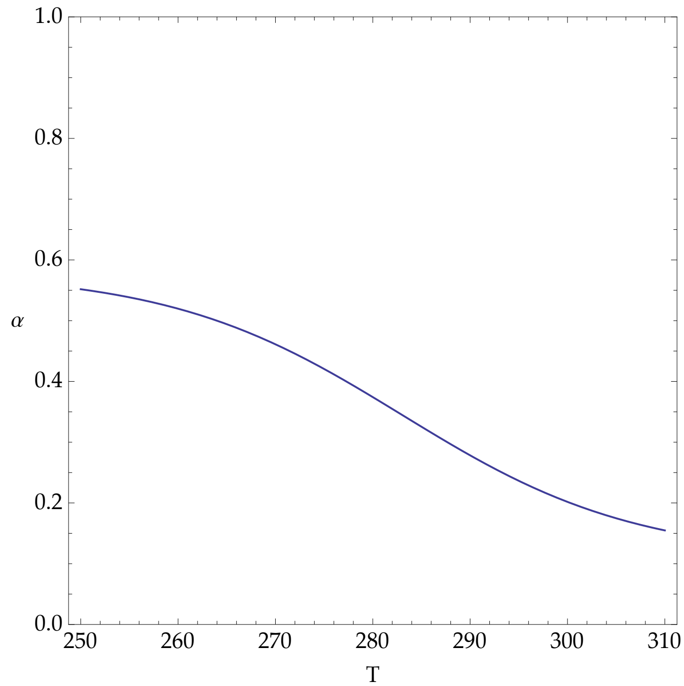

Figure 1: A possible equilibrium planetary albedo due to variations in surface temperature. Here $a_1 = 0.58$, $a_2 = 0.47$, $T^\star = 283$ K, $\Delta T = 24$ K.

Q	Incoming solar radiation	1370 W m^{-2}
h	Height of the atmosphere	10^4 m
ρ_a	Mean density of the atmosphere	1 kg m^{-3}
c_p	Specific Heat Capacity of the Atmosphere	10^3 J kg^{-1} K^{-1}
γ	Greenhouse gas factor	0.6
a_1	Maximum albedo	0.5-0.6
a_2	Albedo parameter	0.4-0.5
$T^\star$		280 K
ΔT		15-20 K
σ	Stefan-Boltzmann's constant	5.67×10^8 W m^{-2} K^{-4}

Table 1: Values of parameters

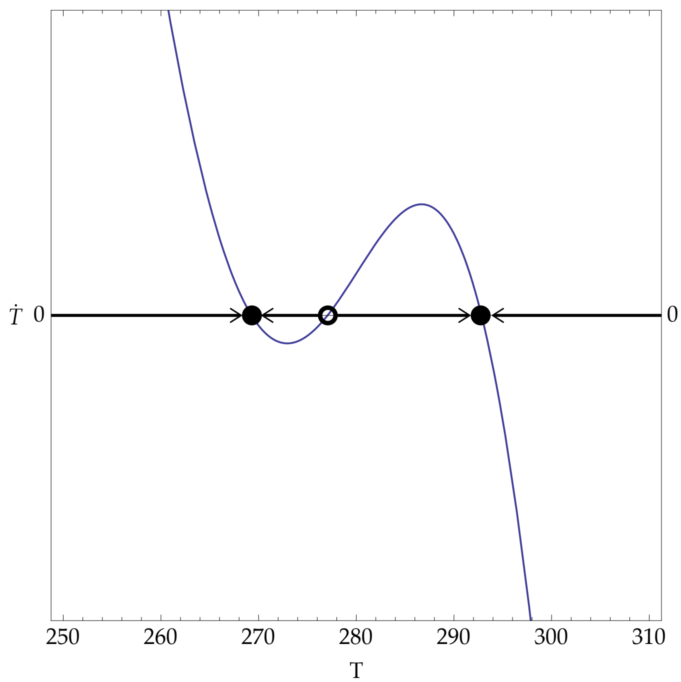

Figure 2: Phase portrait of the system. The filled circles represent stable fixed points, and the open circle represents the unstable equilibrium point. Here $Q = 1370\ \mathrm{W\ m^{-2}}$, $a_1 = 0.58$, $a_2 = 0.47$, $T^{\star} = 283$ K, $\Delta T = 24$ K.

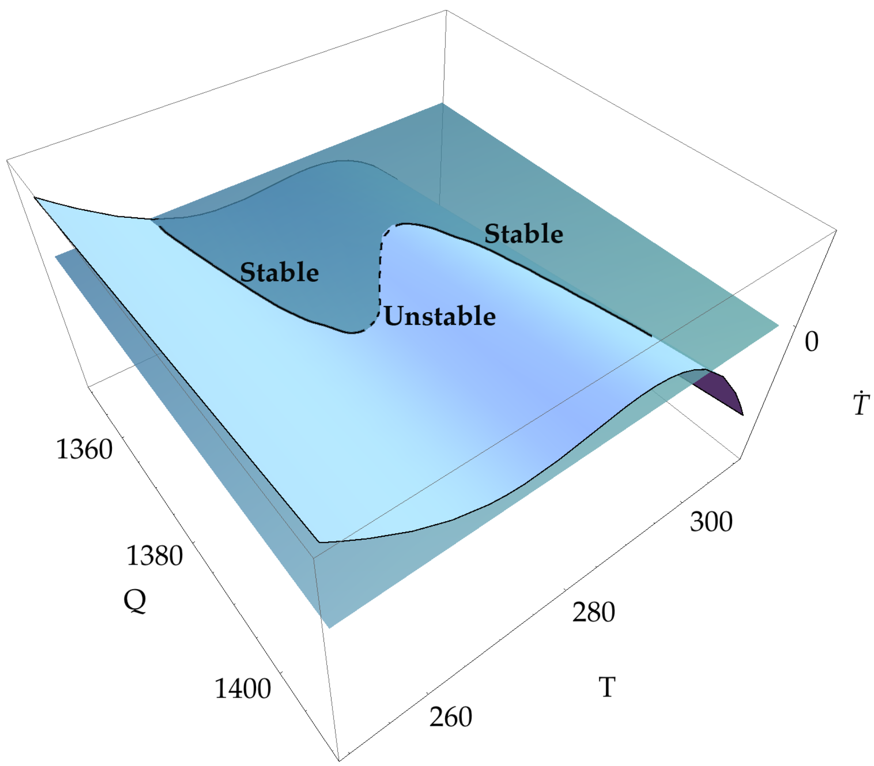

Figure 3: Three-dimensional phase space showing the stable and unstable branches of the system over a range of Q values. The existence multiple-equilibria and hysteresis in this system forms the basis of the Milankovitch theory of ice ages.

1.2 Daisyworld: Watson and Lovelock (1983)

Main idea: Biota and environment are two parts of a coupled system.

Consider an artificial, cloudless planet on which plants of two species - black and white daisies - live. The growth rate of daisies depends on the temperature, which the daisies can modify because they absorb different amounts of sunlight. The growth rates are given by:

$$
\begin{aligned}
\frac{d\alpha_w}{dt} &= \alpha_w(x\beta - \gamma) & (6) \\
\frac{d\alpha_b}{dt} &= \alpha_b(x\beta - \gamma) & (7)
\end{aligned}
$$

where α_w, α_b are the areas covered by white and black daisies and x is the area of the fertile ground not covered by either species, all measured as fractions of the total planetary area. The growth rate of the daisies is β per unit of time and area, and the death rate is γ per unit of time. The area of fertile ground uncolonized by daisies is

$$x = p - \alpha_b - \alpha_w \tag{8}$$

where p is the proportion of the planet's area which is fertile ground.

The growth rate of the daisies is assumed to be a parabolic function of the local temperature T_i:

$$\beta_i = 1 - 0.0032625(22.5 - T_i)^2 \tag{9}$$

The effective temperature at which the planet radiates, T_e, is given by

$$\sigma(T_e + 273)^4 = SL(1 - A) \tag{10}$$

where S has units of flux and L is a measure of the daisyworld's sun's luminosity and A is the albedo of the planet. A is thus

$$A = \sum A_i \tag{11}$$

The local temperatures are defined by introducing a heat transfer coefficient, q.

$$
\begin{aligned}
(T_i + 273)^4 &= q(A - A_i) + (T_e + 273)^4 & (12) \\
&= q(A - A_i) + \frac{SL}{\sigma}(1 - A) & (13)
\end{aligned}
$$

Now if $q = 0$, the situation corresponds to perfect conduction of heat. If $q = SL/\sigma$, then local temperatures are set by local absorption and radiation, with perfect insulation between high and low temperature regions. An intermediate value of $q \sim 0.2SL/\sigma$ is used.

[]

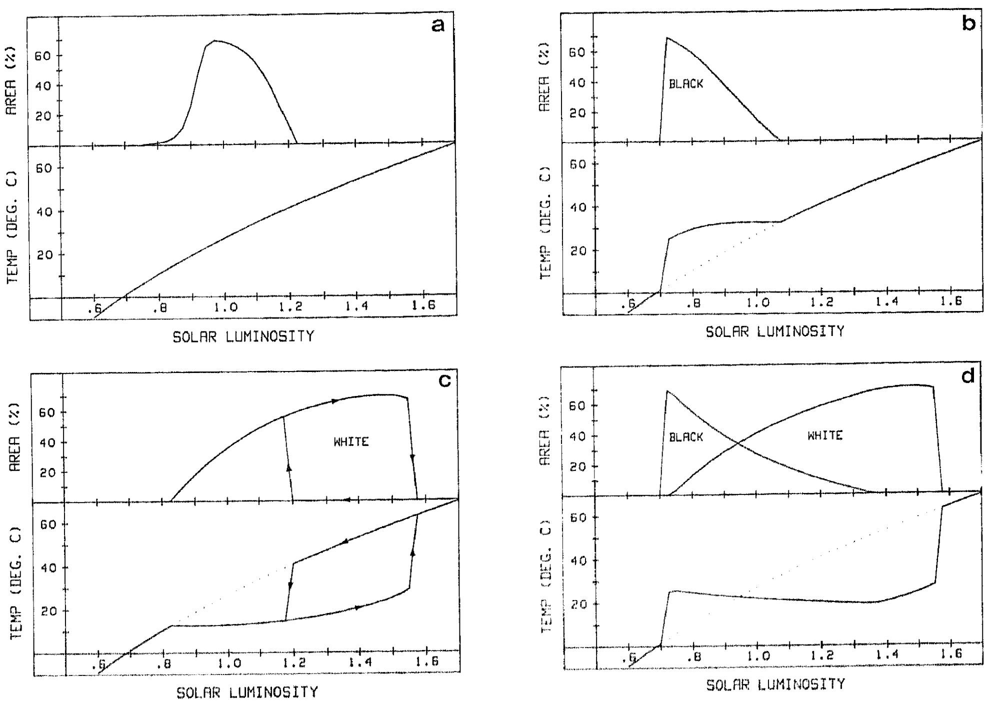

Figure 4:

2 Circulation

2.1 Stommel (2 box)

Heat input into the oceanic surface layers at low latitudes and heat loss at higher latitudes in the North Atlantic results in density driven surface flow. Warmer waters from the tropics flow towards the pole and ultimately sinks due to cooling. On the other hand, evaporation increases the salinity (and hence the density) of low latitude surface waters and thus oppose the density gradient brought about by the temperature gradient. The balance between surface salinity and heat fluxes determine the net direction of meridional flow.

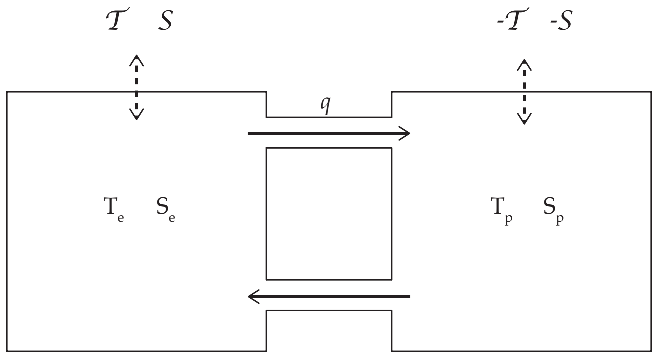

Figure 5: Stommel's two-box model, one equatorial and another polar (subscripts 'e' and 'p' respectively). The water mass in each box is well mixed with uniform temperature and salinities, which relax under prescribed time scales to the imposed surface temperature and salinity forcing. The density difference between the boxes results in the flow of heat and salt.

In the model proposed by Stommel (1961), two boxes, each representing the tropical and polar water columns, are connected via a capillary tube. The boxes are also subjected to surface heat and salt gradients ($\mathcal{T}, \mathcal{S}$ for the tropics and $-\mathcal{T}, -\mathcal{S}$ for the pole). The equations describing the system can then be written as

$$\frac{dT}{dt} = c(\mathcal{T} - T) - |2q|T \qquad (14)$$

$$\frac{dS}{dt} = d(\mathcal{S} - S) - |2q|S \qquad (15)$$

where a single temperature $T = T_e - T_p$ and a single salinity $S = S_e - S_p$ are defined. Quantities c and d represent temperature and salinity transfer coefficients. It is important to note that second terms on the right hand side the flux enters with an absolute value sign. This means that the exchange of properties is insensitive to the direction of circulation. The flow rate q is such that water flows from higher to lower density with a resistance k

$$kq = \rho_e - \rho_p \qquad (16)$$

The flow is positive if directed from the equatorial to the polar box. The counterflow conserves the volume of water in each box.

Density is a function of both temperature and salinity

$$\rho_{[e/p]} = \rho_o(1 - \alpha T_{[e/p]} + \beta S_{[e/p]}) \tag{17}$$

Non-dimensional forms of equations (14, 15) can be written as

$$\frac{dx}{d\tau} = \delta(1-x) - \frac{x}{\lambda}\left| -y + Rx \right| \tag{18}$$

$$\frac{dy}{d\tau} = 1 - y - \frac{y}{\lambda}\left| -y + Rx \right| \tag{19}$$

where $R = (\beta S)/(\alpha T)$ is a measure of the ratio of the effect of salinity and temperature on the density in the final equilibrium state $x = 1, y = 1$. The quantity δ is the ratio of the salinity to temperature transfer coefficients, and λ is the non-dimensional flow strength coefficient. The non-dimensional flow rate f is given by

$$f = \frac{1}{\lambda}(-y + Rx) \tag{20}$$

Equilibrium solutions ($\dot{x} = 0$ and $\dot{y} = 0$) of the system are shown in figure 6. For the chosen parameter values three fixed points a, b and c occur, corresponding to $f = -1.1, -0.3.+0.23$. These represent three different ways in which simple convection can occur between the boxes.

Both a and c are stable equilibrium points. The point b is a saddle point, so that the system would not stay in that state if perturbed ever so slightly.

A similar sketch for the system where only one equilibrium point exists is shown in figure 7.

Dijkstra (2001) provides a good physical description of Stommel's box model along with its three-box extension.

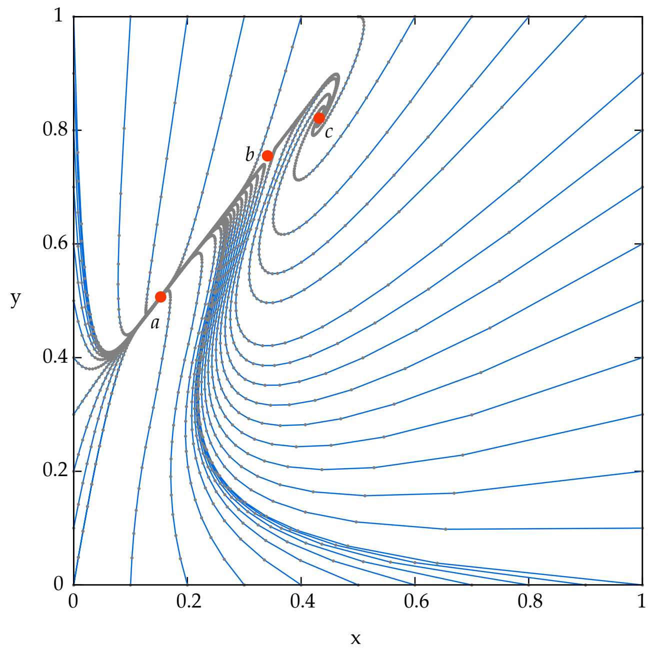

Figure 6: The three equilibria a, b and c (red dots) with $R = 2, \delta = 1/6, \lambda = 1/5$. Several trajectories are drawn from different initial conditions, showing the stable node a, the saddle b, and the stable spiral c.

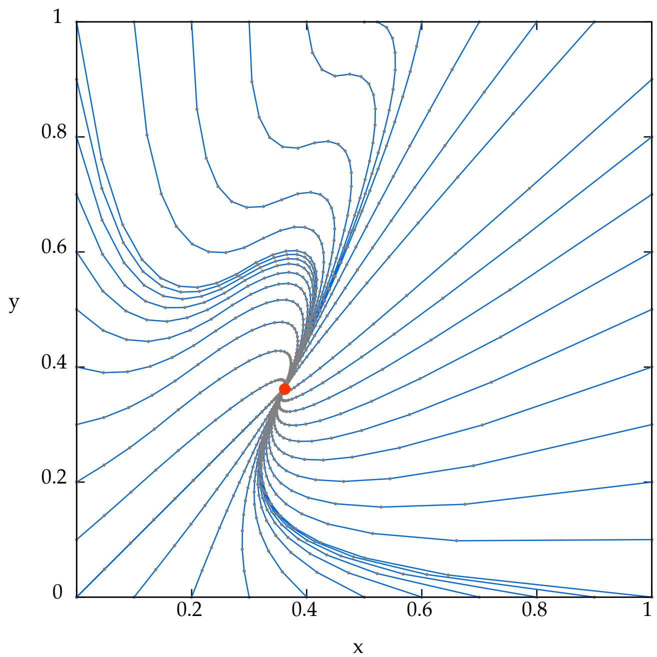

Figure 7: A single stable node is observed for the case $R = 2, \delta = 1, \lambda = 1/5$.

2.2 Stommel (3 box)

The two-box Stommel model can be extended by adding a third box, to have one souther, one equatorial and one northern box. The governing equations can then be re-written to describe the change in temperature and salinity for each box. Four different solutions can thus result, as shown in the figure below:

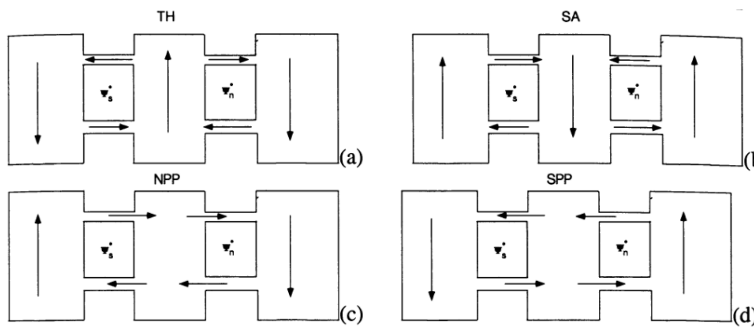

Figure 8:

The bifurcation diagram showing the steady state branches are shown below, under varying values of the surface salinity forcing β (taken to be the same over all the boxes).

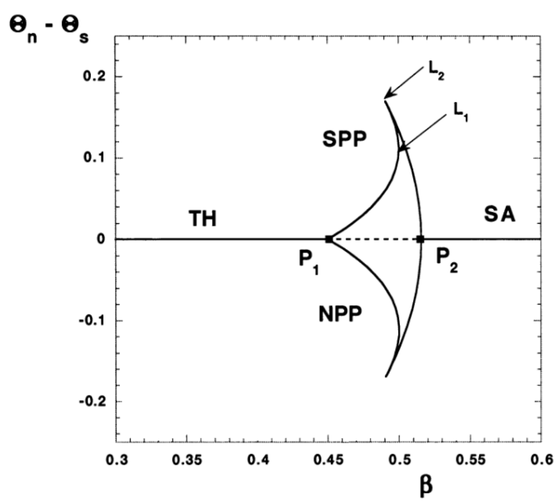

Figure 9:

2.3 Localized Convective Instability:Welander (1982)

Welander (1982) carried out a study of heat and salt exchanges between the atmosphere and oceanic mixed and deep layers using a two-box model. Self-sustained oscillations in heat and salt flow was found between the oceanic layers.

The convective process is highly simplified in this model whereby the rate of turbulent exchange is linearly proportional to the density difference between the two layers, and a step-function is used to prescribe higher mixing rates when stratification is unstable. The model equations are given by:

$$\dot{T} = k_T(T_A - T) - k(\rho)T \tag{21}$$
$$\dot{S} = k_S(S_A - S) - k(\rho)S \tag{22}$$

where the subscript $'A'$ refers to the atmospheric thermal and salinity forcing values. The temperature and salinity of the deep layer is set to zero for simplicity, and k_T, k_S are the thermal and salinity exchange rates between the mixed layer and the atmosphere. Exchange rates between the mixed and deep layer is denoted by $k(\rho)$, which is a positive function increasing monotonically with ρ and having the same values for temperature and salinity Density is prescribed as $\rho = \alpha T + \gamma S$, where α and γ are the thermal expansion and haline contraction rates respectively.

If the relaxation time scale for salinity is larger than that of temperature, the system may become unstable and go into self-sustained oscillations.

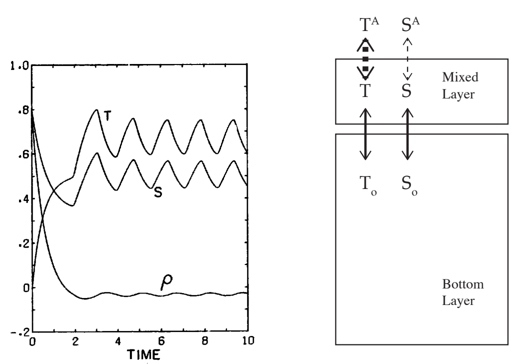

Figure 10:

3 Ocean - Atmosphere

3.1 Wigley & Schlesinger 1985

Main idea: Four boxes, two of which are atmospheric, and two vertical oceanic layers. One of the atmospheric boxes is over land.

The rate of change of temperature of the mixed layer is given by:

$$C_m \frac{d\Delta T}{dt} = \Delta Q - \lambda \Delta T - \Delta M \tag{23}$$

where C_m is the total heat capacity of the mixed layer, ΔT is the temperature difference due to perturbations at i) the surface from change in surface thermal forcing, ΔQ; ii) the atmospheric feedback expressed in terms of a feedback parameter, λ; iii) and leakage of heat into the deep layers, ΔM.

The energy flux at the boundary of the mixed and deep layer, ΔM, acts as an upper boundary condition for the deep ocean in which the turbulent diffusion coefficient, K, is taken to be a constant. The equation describing the rate of change of temperature of the deep ocean is given by:

$$\frac{\partial \Delta T_o}{\partial t} = K \frac{\partial^2 \Delta T_o}{\partial z^2} \tag{24}$$

Assuming a continuity at the interface between the mixed layer temperature change, ΔT, and the deeper-layer temperature change evaluated at the interfacial level, $\Delta T_o(0, t)$,

$$\Delta T_o(0, t) = \Delta T(t) \tag{25}$$

The value of ΔM can be calculated using:

$$\Delta M = -\frac{C_m}{h} K \left[\frac{\partial \Delta T_o}{\partial z} \right] \Bigg|_{z=0} \tag{26}$$

where h is the depth of the mixed layer.

This model can be used to investigate the effects of changing atmospheric forcings, ΔQ: either with an instantaneous jump or through a gradual change.

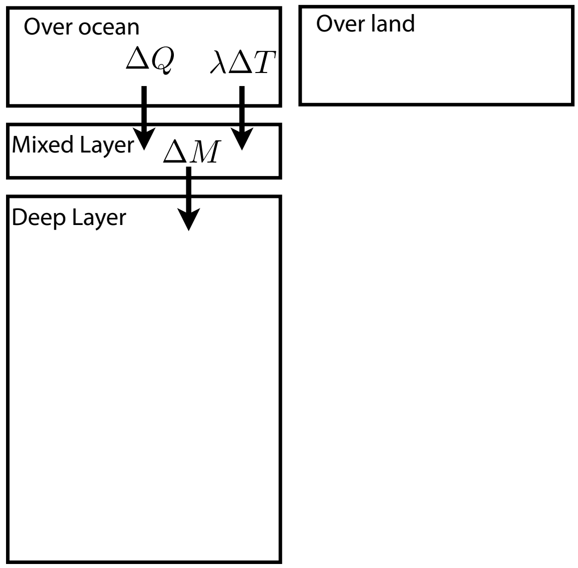

Figure 11:

If the deep ocean is assumed to be infinitely deep, ΔM can be written as:

$$\Delta M = \mu C_m \frac{\Delta T}{(\tau_d t)^{1/2}} \tag{27}$$

where μ is a tuning parameter (from comparing the full numerical solution with the approximation), and $t_d (= \pi h^2/K)$ is the characteristic time for exchange between the mixed and deep layers. Using the above, the system then becomes an ODE:

$$C_m \frac{d\Delta T}{dt} = -\Delta T\left(\lambda + \frac{\mu C_m}{(\tau_d t)^{1/2}}\right) - \Delta Q \tag{28}$$

[GET FIGURES]

4 Carbon Cycle

4.1 Glacial Cycles and CO_2: Hogg (2008)

In this model, radiative balance is combined with greenhouse gas effects. The ocean is made reservoir for CO_2 and its release into the atmosphere is made dependent on the rate of change in global temperatures.

A simple radiative balance of the earth can be written as

$$\overline{S} + \overline{G} = \sigma T^4 \tag{29}$$

where $\overline{S}$ is the mean incoming solar radiation, $\sigma = 5.67 \times 10^{-8}$ W/m^2/K^4 is the Stefan-Boltzmann constant and $\overline{T}$ is the global mean temperature. The rate of change of temperature can then be written as

$$c\frac{dT}{dt} = S + G - \sigma T^4 \tag{30}$$

where c is the specific heat capacity of the ocean, and S, G and T are allowed to vary in time.

The greenhouse gas forcing is varied as

$$G(t) = \overline{G} + A\ln\left(\frac{C(t)}{C_o}\right) \tag{31}$$

where $C(t)$ is the atmospheric concentration of CO_2 and C_o is the preindustrial concentration. Putting together other sources and sinks for carbon, the following relation for the rate of change of carbon in the atmosphere is obtained:

$$\frac{dC}{dt} = V - (W_o + W_1 C) + \beta(C_{\max} - C)\max\left(\frac{dT}{dt} - \epsilon, 0\right) \tag{32}$$

The first term on the RHS is a constant volcanic source. The second term represents a weak sink due to silicate weathering of rocks. The last term represents a release of CO_2 with significant warming, *i.e.* $\frac{dT}{dt} > \epsilon$, and is limited to a value of $C_{\max}$, whose value is chosen to simulate observed glacial-interglacial ranges. The parameter ϵ is dependent on the timescale of the orbital forcing.

The temperature equation can be expressed as:

$$\frac{dT}{dt} = S(t) + \overline{G} + A\ln\left(\frac{C(t)}{C_o}\right) - \sigma T^4 \tag{33}$$

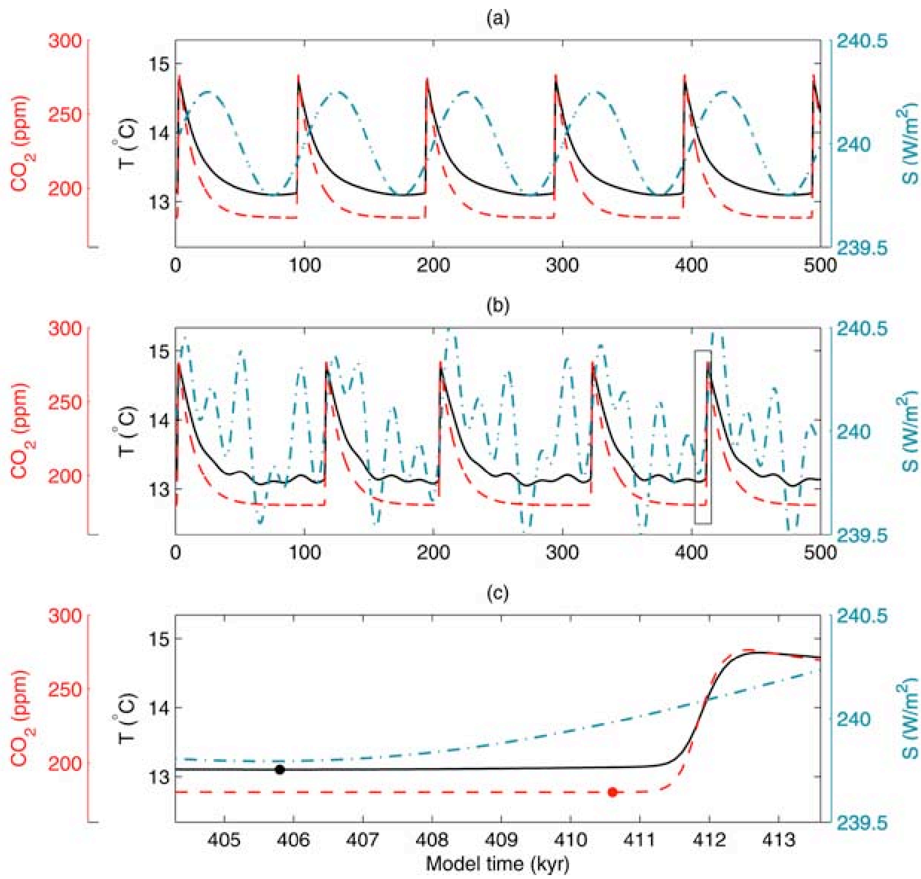

Figure 12:

The pair of coupled ODEs given above describe the climate system. Glacial-interglacial switches are observed if $S(t)$ is made to vary sinusoidally to simulate Milankovitch cycles.

References

Dijkstra, H. *Nonlinear Physical Oceanography: A Dynamical Systems Approach to the Large Scale Ocean Circulation and El Niño*. Springer, 2001.

Hogg, A. Glacial cycles and carbon dioxide: A conceptual model. *Geophysical Research Letters*, 35, 2008.

Stommel, H. Thermohaline convection with two stable regimes of flow. *Tellus*, 1961.

Watson, A. and Lovelock, J. Biological homeostasis of the global environment: the parable of daisyworld. *Tellus*, 35B:284, 289 1983.

Welander, P. A simple heat-salt oscillator. *Dynamics of Atmosphere and Oceans*, 6(233-242), 1982.